Geochemical Journal, Vol. 21, pp. 11 to 21, 1987

Hydrothermal activity on the summit of Loihi Seamount, Hawaii

H. SAKAI[1], H. TSUBOTA[2], T. NAKAI[1], J. ISHIBASHI[1], T. AKAGI[3], T. GAMO[1], B. TILBROOK[6], G. IGARASHI[4], M. KODERA[4], K. SHITASHIMA[2], S. NAKAMURA[5], K. FUJIOKA[1], M. WATANABE[1], G. MCMURTRY[6], A. MALAHOFF[6] and M. OZIMA[4]

Ocean Research Institute, University of Tokyo, Nakano-ku, Tokyo 164[1], Faculty of Integrated Arts and Sciences, Hiroshima University, Naka-ku, Hiroshima 730[2], Department of Chemistry, University of Tokyo, Bunkyo-ku, Tokyo 113[3], Department of Geophysics, University of Tokyo, Bunkyo-ku, Tokyo 113[4], Muroran Institute of Technology, Muroran 050, Japan[5], and Department of Oceanography and Hawaii Institute of Geophysics, University of Hawaii, 1000 Pope Rd., Honolulu, HI 96822, U.S.A.[6]

(Received December 5, 1986: Accepted January 14, 1987)

Oceanographic studies including CTD survey of warm sites and bottom photography confirmed several hydrothermal fields on the summit of Loihi Seamount, Hawaii. Warm water venting at these sites forms chimneys sticking out of and veins cutting through older precipitates. The summit is covered with hydrothermal plumes which are extremely rich in methane, helium, carbon dioxide, iron and manganese, the maximum concentration of helium being 91.8 nl/l, the highest so far reported for open-ocean water. The $^3He/^4He$ ratio of helium injected into seawater is 14 times the atmospheric (1.4×10^{-6}) and similar to that reported for Kilauea and other hotspot-volcanic gases. The ^3He/heat and CO_2/heat ratios in the plume are one to two orders of magnitude greater than those at oceanic spreading centers, implying a more primitive source region for hotspot volcanism. The Loihi plumes show negative pH anomalies up to half a pH unit from ambient owing to the high injection rate of CO_2.

INTRODUCTION

Loihi Seamount is located about 30km southeast of the Island of Hawaii (Fig. 1 insert). It rises from the sea floor at a depth of 4,000m and reaches a maximum elevation of 1,000m below sea level. The summit of the volcano contains a 2 by 4km wide caldera-like depression with steep inner and outer walls (Fig. 1, Malahoff *et al.*, 1982). Bottom photography and dredging (Malahoff *et al.*, 1982; Moore *et al.*, 1982; De Carlo *et al.*, 1983) have indicated that fresh lava flows and associated hydrothermal deposits occur abundantly within and around the summit. Fields of hydrothermal chimneys have also been photographed (Malahoff, 1986). The hydrothermal deposits are mixtures of nontronite (Fe-rich smectite) and goethite (De Carlo *et al.*, 1983). Water temperature anomalies of up to 1°C above ambient have been recorded at a depth of 10m above the bottom in areas where hydrothermal precipitates occur (Malahoff *et al.*, 1982). Results of previous studies suggest that active hydrothermal fields similar to those found at the mid-ocean ridges also exist on the Loihi summit. In order to obtain more direct evidence of hydrothermal activity, the "Delphinus Expedition" visited Loihi Seamount on 6-10 September 1985, in the University of Tokyo research vessel (R/V) Hakuho Maru. The distribution of methane, helium and its isotopic ratio, and selected trace heavy metals in the water column above the summit was measured as geochemical indicators of hydrothermal emissions (Lupton *et al.*, 1977; Welhan and Craig, 1979). Bottom temperature anomalies over the summit area were surveyed by a Neil Brown CTD tow system. Bottom features around the sites of temperature anomaly were photographed by a deep sea camera. This report presents the

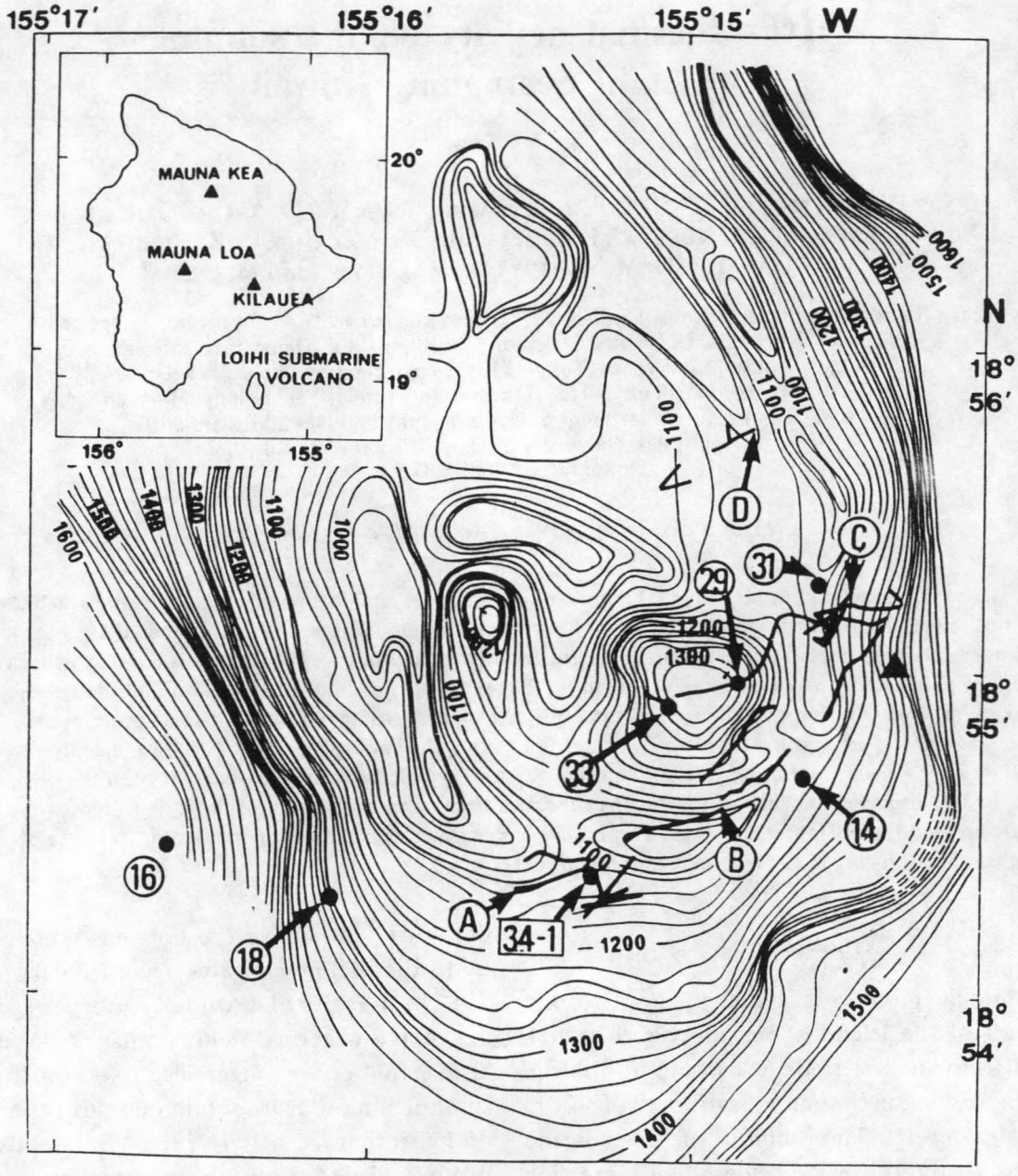

Fig. 1. Topographic map of the Loihi summit area showing traces of the CTD tow (solid lines), localities of temperature anomaly (circled capital letters), and hydrocast stations (circled numbers). Map modified after Malahoff (1986). Contours are in meters. The number within the box rectangle marks a water sampling site along the CTD tow. Of eight sampling sites, only the single site noted in the text is shown.

general results that confirm active hydrothermal activity on the Loihi summit and discusses some features that distinguish the Loihi hydrothermal activity from those of mid-ocean ridge. More detailed discussion on the chemical nature of Loihi hydrothermal emission based on methane distribution will be given elsewhere (Gamo, Ishibashi and Sakai, in preparation).

Experiental

The CTD system was towed horizontally within the summit caldera and its adjacent area at depths less than 10m above the sea-floor. During the CTD tow, conductivity (in salinity, ±0.003), temperature (±0.001°C), and depth (in

decibar, ±0.1) were continuously recorded and displayed in real-time on board. The ship's position was determined within ±20m relative to the smaller summit pit crater (Fig. 1) with a Motorola Mini-Ranger Falcon IV navigation system. False temperature anomaly spikes due to water mixing or vertical movement of the CTD vehicle were eliminated by using the procedure of Weiss *et al.* (1977), as will be described later. When temperature anomalies were detected, Teflon-coated 5-litre Go-Flo (General Oceanics) samplers attached to the frame of the CTD vehicle were activated to obtain water samples that could be analyzed for indications of hydrothermal activity. Bottom photography of the temperature anomaly sites was taken with a Benthos 372 twin camera and a 382 electroflash.

The vertical distribution of methane, helium and its isotopic ratio, and trace heavy metals in the water column above the summit area were studied by hydrocasts with 23-litre Niskin-type bottles. In addition, two types of clean water samplers, CIT-type (Schaule and Patterson, 1981) and TMK-type were used to collect samples for ultratrace heavy metal analyses at selected sites and depths. The latter is a ten litre bellows-type polyethylene water sampler which has been proven to be as clean as the CIT-type (Tsubota, Murozumi and Kanamori, in preparation). Methane, together with pH, titration alkalinity (TA) and nutrients (Si, NO_3, PO_4), were analyzed on board, whereas helium, trace heavy metals and total dissolved inorganic carbon (ΣCO_2) in land-based laboratories. All these analyses were performed on unfiltered samples according to the procedures described below.

Methane was flushed out of 500ml seawater with helium immediately after it was brought on board and analyzed with a FID gas chromatograph. The technique was essentially a modification of that of Kim (1983) and Lilley *et al.* (1983), and will be described in more detail in an accompanying paper (Gamo, Ishibashi and Sakai, in preparation). Poisoned aliquots of the same water samples were brought to the Department of Oceanography, University of Hawaii and analysed for methane similarly. The results were in excellent agreement with the shipboard analyses reported here. Helium was analyzed on seawater clamp-sealed into 40ml copper tubings immediately after it was brought on board. For detailed analytical procedures, refer to Sano *et al.* (1985). The $^3He/^4He$ ratio was expressed in R/R_A, where R and R_A (= 1.4×10^{-6}) are the isotopic ratio of sample and atmospheric helium, respectively. Air contamination in the helium analyses, as estimated from the ^{20}Ne content in each sample, is 20 ± 20% of the ^4He found in two samples at station 33 (970 and 1,063m depths) and 10 ± 10% in others. The large uncertainty in the estimation is due to the instrumental instability during neon peak measurements. It allows us only to set the maximum level of contamination and therefore limits the accuracy of the helium isotope ratios, although it does not affect the following discussion.

Trace heavy metals were analyzed with an ICP emission spectrometer after they were concentrated by coprecipitation with gallium hydroxide (Akagi *et al.*, 1985). pH and TA were analyzed by a glass pH electrode and by an automatic titrator, respectively. ΣCO_2 was determined by a gas chromatographic technique developed by Gamo and Horibe (1980) on poisoned seawater kept in air-tight glass bottles.

Results

Figure 1 is a topographic map of the Loihi summit area showing the traces of the CTD tows, the locations of temperature anomalies detected and their associated seawater sampling sites, and the hydrocast station. Figure 2 shows a real time record of temperature (T°C), salinity (S), and depth (P decibar) obtained when the CTD vehicle passed over site A (Fig. 1) at a water depth of within 10m above the bottom. In the water column above this station, a linear relationship holds: $T = -12.522S + 436.303$. Therefore, $T + 12.522S$ plot in Fig. 2 (the 3rd from top indicated as T + S) should be invariant

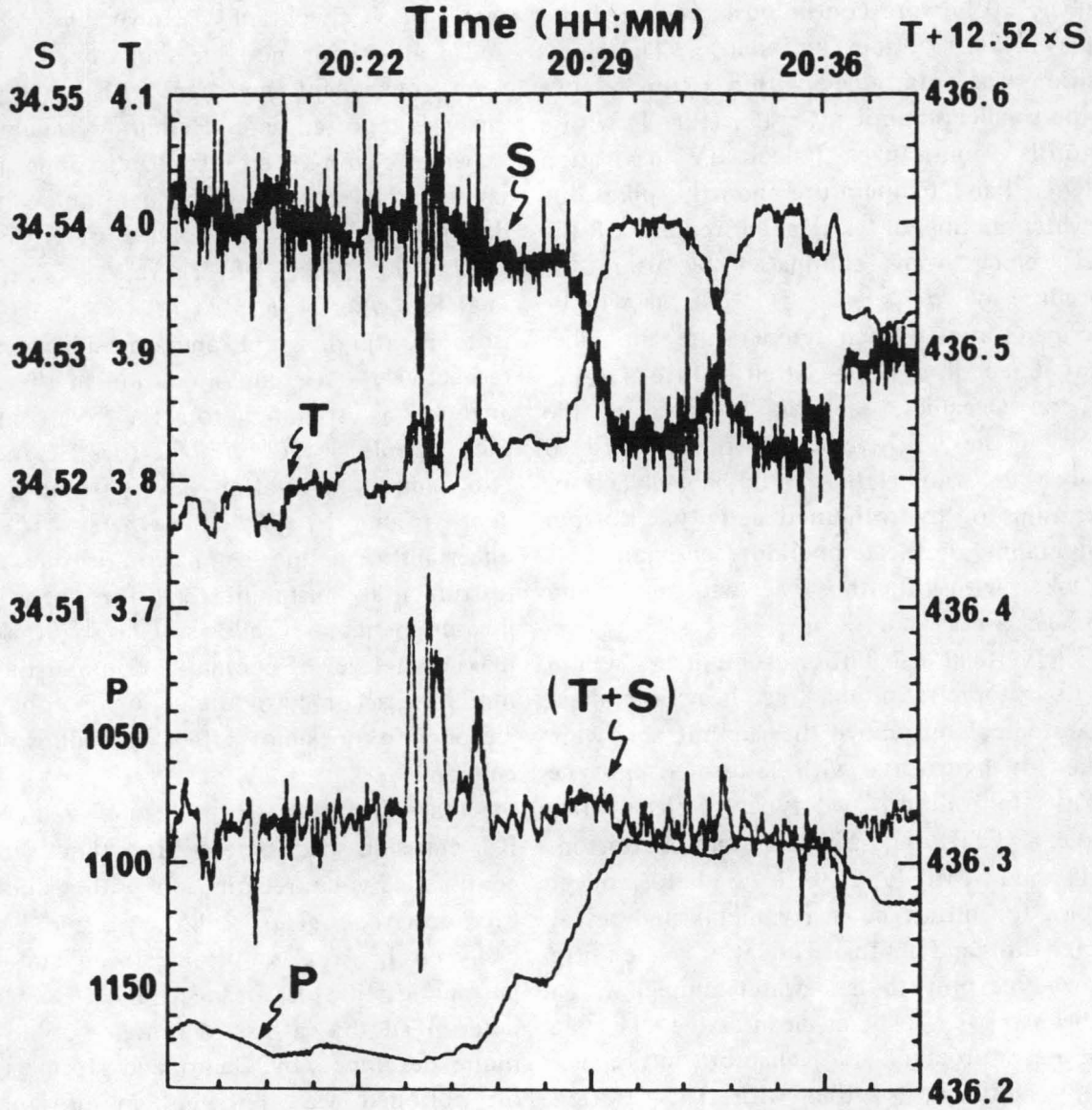

Fig. 2. An example of the CTD record showing time-variation of salinity (S), temperature (T°C) and water depth (P in decibar) when the CTD vehicle passed over site A of Fig. 1. (T + S) is a plot of "T + 12.522 × S". The positive spikes on the plot indicate temperature anomaly due to injection of warm water into ambient seawater. For details, see text.

to temperature variation due to up-down movement of the CTD vehicle and to local vertical mixing of water masses. Deviation from the linear relationship was taken to be true temperature spikes due to warm water mixing (Weiss *et al.*, 1977). Figure 2 reveals that several true temperature spikes occur between 20h 22min to 24min, the maximum being about + 0.07°C. The minimum temperature anomaly that may be detected by this system would be 0.02°C. Note also that the large temperature spikes between 20h 29min to 36min was due to a 50 meter uplift of the CTD vehicle and disappeared on the T + S plot. Four warm spots were found during the study (Fig. 1). One on the northern floor in the caldera-like depression (D) with a temperature anomaly of +0.025°C and three along the southern and eastern caldera rim (A, B and C) with maximum anomalies of +0.07, +0.05, and +0.04°C, respectively. In the latter three areas, fresh pillow basalt flows and hydrothermal deposits had been identified by dredging

and bottom photography (Malahoff *et al.*, 1982; Malahoff, 1986) and were similarly confirmed by the present cruise (see below). The northern warm spot, however, was not reported by the previous studies.

Depth profiles of methane analyzed on board and trace heavy metals at stations 29 and 33 are shown in Fig. 3 together with their pH, total inorganic carbon, and titration alkalinity. Six samples from station 33 have also been analyzed for helium isotopes and the results are included in Fig. 3. Seawater samples at station 29 were collected with 23-litre Niskin-type bottles. At station 33, seawater for the analyses of heavy metals was taken by the CIT - and TMK - samplers, whereas that for other components was collected in 23-litre Niskin-type bottles, which were set about 2m above the clean samplers at corresponding depths of a single cast. Nickel and cobalt (not presented) did not show any anomalies at station 33. ΣCO_2 was not measured at station 33.

These results indicate that about 150m-thick water layers exist at a depth of 100 to 150m above the summit floor which are highly enriched in methane, helium with high $^3He/^4He$ ratios, and certain heavy metals. It should also be noted that the methane-rich waters generally show a negative pH anomaly. A strong correlation among these components, except for nickel and cobalt, is also notable. Two anomaly peaks appear for methane, iron, and manganese at station 29 and for ^3He and probably for methane at station 33. Their presence implies that there are at least two types of active vents which emit fluids of somewhat different nature. Although not shown, iron and manganese also covary with each other at station 31, showing peak concentrations at a water depth of 1,020m, although no anomaly was detected for nickel and cobalt. Except for station 16, methane at all other stations showed nearly the same depth profiles as those in Fig. 3 with values ranging from 180 to 330nl/l. Helium and heavy metals were not measured at these stations. Station 16 showed no anomaly.

The methane content and helium isotope ratio (in R/R_A) in 8 water samples collected

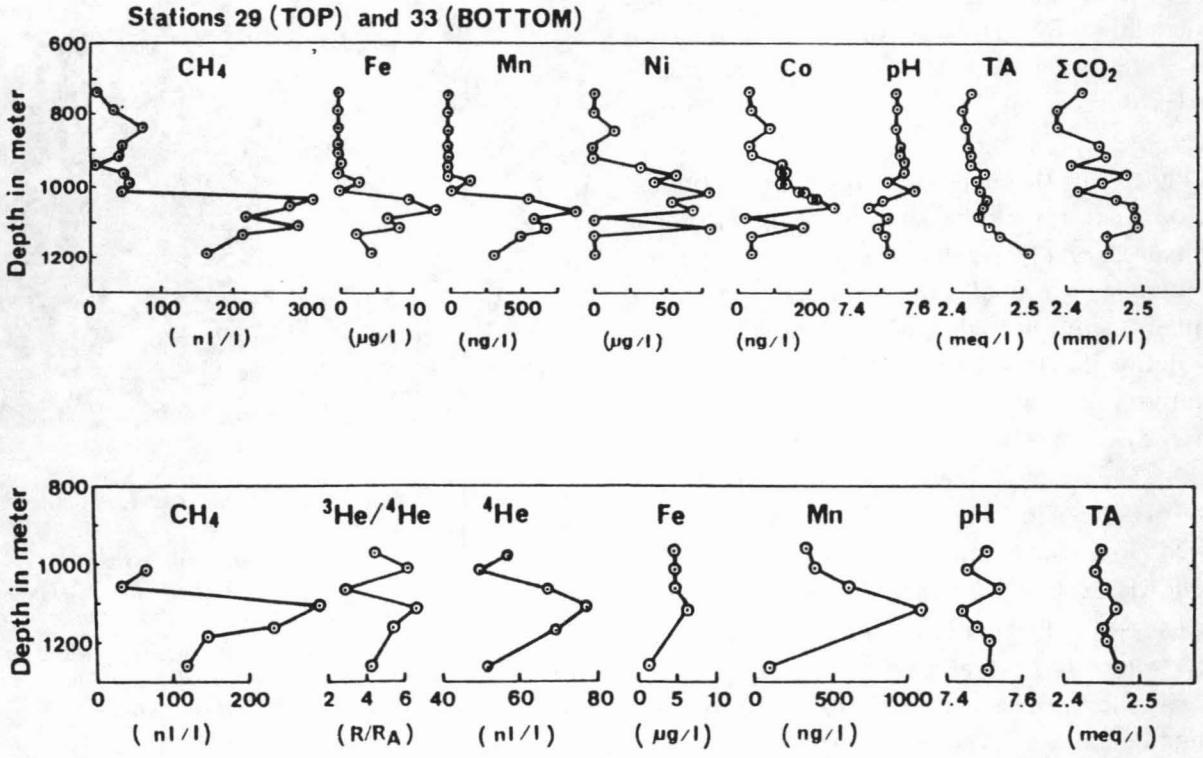

Fig. 3. Vertical distribution of hydrothermal effluents in the water column at stations 29 (top) and 33 (bottom).

during the CTD tows ranged from 100 to 585 nl/l and from 3.0 to 11.3, the highest values both being found in water sample 34-1 collected in the vicinity of warm site A (Fig. 1). This water has a helium content of 91.8 nl/l and a pH of 7.18, the highest helium and pH anomalies so far reported for open-ocean water. Unfortunately, however, sampling seawater with the CTD vehicle at all the sites of temperature anomaly failed due to loss of Go-Flo bottles or to failure in activating the sampling device in time. Therefore, any precise relationship between ^{3}He content and water temperature could not be obtained.

The nickel and cobalt anomaly at station 29 is too large to result from any possible contamination from the Niskin bottles employed there. During the hydrocast at station 29, for example, seawater at about 5 m below the lowest Niskin bottle was taken with the CIT-type clean sampler. The concentration of nickel and cobalt in this sample is 600 ± 100 and 40 ± 10 ng/l, respectively, compared with 970 and 40 ng/l in the overlying water taken with the Niskin bottle. This example and our previous experience in heavy metal analyses in seawater (Akagi and Haraguchi 1984) indicate that the contamination level of nickel and cobalt from Niskin bottles is less than 200 ng/l and 30 ng/l, respectively.

Plates 1 through 3 show three typical bottom features at the sites of temperature or methane anomaly: yellowish- to reddish-brown sediments with small chimneys (plate 1), dark sediments cut through with yellow veins (plate 2), and yellowish- to reddish-brown sediments underlying pillow debris coated with sediments (plate 3). The first photo was taken nearby station 14, whereas the other two in the proximity of site A in Fig. 1. The chimneys do not exceed 30 cm in height and some of them have a yellowish round top with a small hole. These photos probably represent Loihi hydrothermal fields where warm water emerges through veins and chimneys. The yellowish- to reddish-brown sediments may consist of nontronite (iron-rich smectite) and goethite, as reported by De Carlo *et al.* (1983).

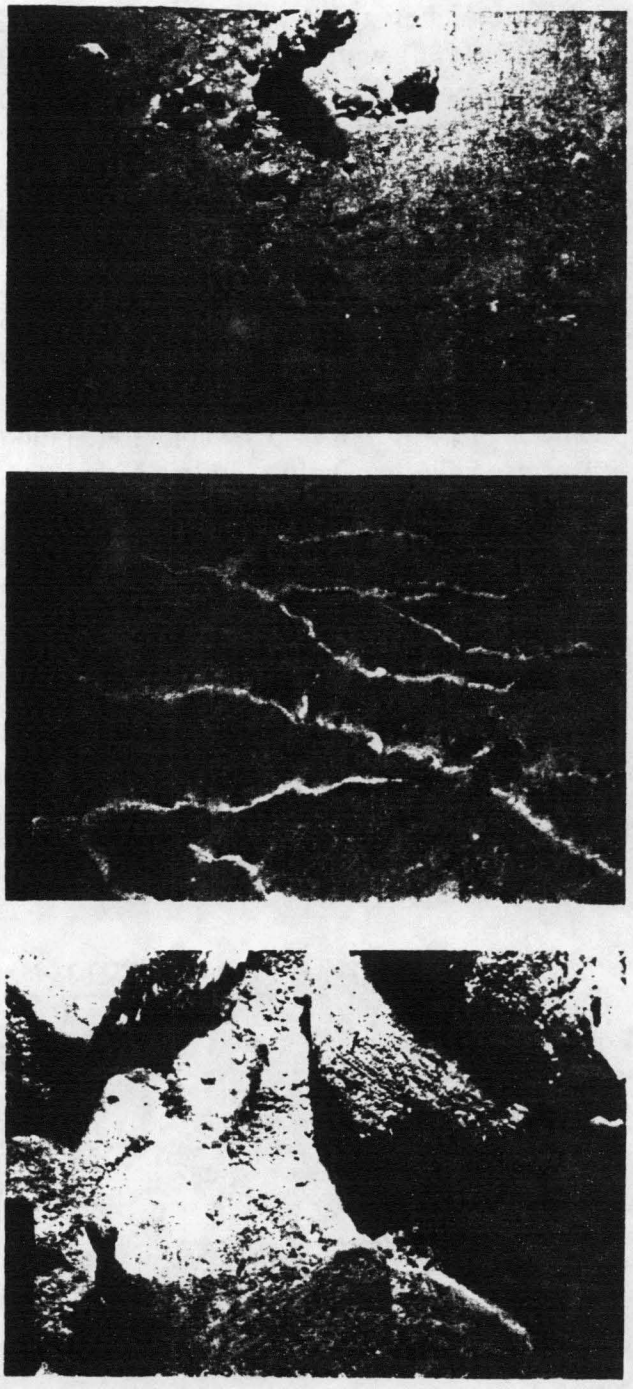

Plates 1–3. Bottom features on the Loihi summit suggesting hydrothermal activity.
1: Chimneys sticking out of sediments which cover an area near station 14 in Fig. 1. The heights of the two largest chimneys are about 30 cm. Note a hole on the top of one of the chimneys which may be or was a conduit for warm water. Photo-coverage 1.2 × 1.5 m.
2: Yellow veins cutting through dark sediments nearby site A. Warm water may be issuing through the veins. Photo-coverage 1 × 1.3 m.
3: Reddish-brown sediments underlying pillow basalt debris. Photo-coverage 0.6 × 0.74 m.

Discussion

Figure 4 plots the concentration of ^3He against those of CH_4 and ^4He, respectively, in water samples from station 33 and sample 34-1. Because of difficulty encountered in the correction of the helium data (see the section of "Experimental"), values uncorrected for possible air contamination are plotted in Fig. 3. The slope of the line connecting the ambient seawater and the sample waters represents the methane/^3He and $^3He/^4He$ ratios of the end-member fluid injected into the ambient seawater, respectively. The estimated ratio of methane to helium-3 is 4.7×10^5 (line A, Fig. 4) and is in accord with the values of 2×10^5 previously reported for the plume at Easter Island and Loihi (Craig *et al.*, 1984; Horibe *et al.*, 1983). As have been noted by the above authors, these values, however, are more than one order of magnitude smaller than the ratios in the Galapagos Ridge (GR) and 21°N East Pacific Rise (EPR) hydrothermal fluid (Welhan and Craig, 1983; Lilley *et al.*, 1982).

The $^3He/^4He$ ratio (R/R_A) of the injected helium shows a wide variation from 21.5 to 5.0 (lines B and D, Fig. 4). The point on line D which represents a 1063 m-deep water sample from station 33 is suspected to contain a larger amount of air contamination than the others. Disregarding this suspected sample, the range shrinks to 21.5 to 10, averaging 14 (line C) which is similar to that typically observed in volcanic gases from hotspot volcanoes: Kilauea (R/R_A = 15, Craig and Lupton, 1976), Yellowstone (15.6, Craig *et al.*, 1985), and Geysir, Iceland (16, Sano *et al.*, 1985). This range is significantly greater than that from hydrothermal vents at GR and 21°N EPR (7 ~ 8, Welhan and Craig, 1983; Jenkins *et al.*, 1978). The average ratio is slightly larger than that of helium which is being injected into the hydrothermal plume at Easter Island (Craig *et al.*, 1984). The R/R_A of helium extracted from the Loihi basalt glasses, however, displays a wide range of variation from 20 to 32, with alkalic basalts generally showing lower values than the tholeiitic ones (Kurz *et al.*, 1983; Rison and Craig, 1983). If the maximum possible air contamination in helium analyses of seawater samples is taken to be 20% as was mentioned before, the slopes of lines B and C could be increased by a factor of 1.25 and could overlap with the lower range of the basaltic values. However, a more accurate correction for air contamination is needed to explain the difference in the isotopic ratio between the plume and basalt values and the wide variation of the ratio within each group.

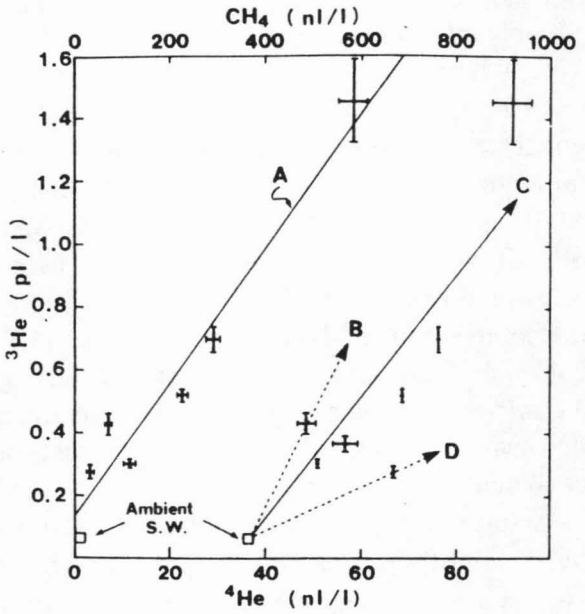

Fig. 4. ^3He versus CH_4 and ^3He versus ^4He relationships in samples at station 33 and sample 34-1. Line A is the least square fit to ^3He versus CH_4 data points. Line C represents the average $^3He/^4He$ slope between each sample point and the ambient seawater, which is a 1000-m-deep water sample about 50 km east of Loihi and has a R/R_A of 1.24 ± 0.10. The point on line D is excluded in the calculation of line C because of its larger uncertainty in air contamination than others (see the section of "Experimental"). The slopes of lines are:
A = $^3He/CH_4 = 2.11 \times 10^{-6}$ ($CH_4/^3He = 4.7 \times 10^5$)
B = $^3He/^4He = 30.1 \times 10^{-6}$ ($R/R_A = 21.5$)
C = $^3He/^4He = 19.5 \times 10^{-6}$ ($R/R_A = 13.9$)
D = $^3He/^4He = 7.0 \times 10^{-6}$ ($R/R_A = 5.0$)

The low pH value of the methane-rich samples may be caused by strongly acid hot water that is being injected into ambient seawater. Similar acid end-members have been found at mid-ocean ridge hydrothermal vents

(Michard *et al.*, 1984). If the buffering capacity of ambient seawater against H^+ is assumed to be 4×10^{-4} mol/l/unit pH (Skirrow, 1974), then 2×10^{-4} mol of hydrogen ion must be added to one litre of ambient seawater of pH = 7.6 in order to lower its pH by half a unit. Such an addition would, however, also lower the alkalinity of the seawater by 0.2 meq/l or 8 percent of an ambient value (2.45 to 2.50 meq/l). On the contrary, the alkalinity of sample 34-1 is 2.451 meq/l and does not show such a decrease. At any other sample localities (Fig. 2) methane-rich seawater does not show a resultant decrease in alkalinity.

Alternatively, the pH drop may be caused by the addition of carbon dioxide. The buffering capacity of seawater against CO_2 is nearly the same as that against H^+ (Skirrow, 1974), but the pH change occurs without any change in alkalinity. The methane-rich water sampled at station 29 has pH values about 0.1 unit lower than ambient seawater which at constant alkalinity would require the addition of 4×10^{-5} mol CO_2/l of water. This is in agreement with the observed excess total inorganic carbon of 5×10^{-5} mol/l in this water layer (Fig. 3 top). Because the methane content of these samples is approximately 300 nl/l or 1.3×10^{-8} mol/l, the methane/excess carbon dioxide molar ratio in the original fluid should have been about 3×10^{-4} if no appreciable loss of methane had occurred since mixing into seawater. Similarly in sample 34-1 the methane/excess carbon dioxide ratio should be about half that estimated for samples from station 29. From these values and the methane/helium-3 ratio previously estimated, the excess carbon dioxide/helium-3 ratio is calculated to be 1 to 3×10^{-9}.

Table 1 summarizes the abundances of excess methane, carbon dioxide and manganese relative to the excess helium-3 in the Loihi plume and compares them with those found in hydrothermal fluids at Easter Island, GR and 21°N EPR. The Loihi plume is nearly two orders of magnitude more enriched in ^{3}He relative to methane and manganese than those at the mid-ocean ridge hydrothermal sites. As mentioned before, the same is also true for methane in the Easter Island plume. At the Galapagos hydrothermal system, a heat/^{3}He ratio of 7.6×10^{-8} cal/atom has been estimated (Jenkins *et al.*, 1978). If this ratio is applied to the present results, the plume samples collected at station 33 should have had temperature more than 1°C higher than ambient seawater, however, no such large temperature anomaly was recorded during any passage of the CTD through the methane-rich water layers. These facts clearly demonstrate that the rate of helium emission, both ^{3}He and ^{4}He, for a given heat flux at Loihi Seamount and possibly also at Easter Island is one to two orders of magnitude greater than at GR and 21°N EPR. Because the excess carbon dioxide to helium-3 ratio in the Loihi plume is nearly the same as that in the other two areas (Table 1), the same can be said of the excess carbon dioxide/heat ratio. This large excess carbon dioxide/heat ratio explains the reason why the pH anomaly is observed in the Loihi plume, whereas no such pH anomaly has been reported in association with helium and methane anomalies in plumes above GR and 21°N EPR.

Kaneoka and Takaoka (1980) predict that the source region for Hawaiian volcanism is more primitive and enriched in volatiles and incompatible components than that for the

Table 1. Abundances of excess methane, manganese and carbon dioxide relative to excess helium-3 in hydrothermal plumes at Loihi and Easter Island and in vent fluids at GR and 21°N EPR

	Loihi	Easter Is.	GR	21°N EPR
$CH_4/^3He$ ($\times 10^5$)	4.7	1.9*[1]	120, 150, 420*[2]	35, 65*[3]
$Mn/^3He$ ($\times 10^5$)	1.4-11	–	650-1700*[4]	430*[4]
$CO_2/^3He$ ($\times 10^9$)	1-3	–	1*[5]	0.5-0.6*[6]

*[1] *Craig et al. (1984);* *[2] *Lilley et al. (1983);* *[3] *Welhan and Craig (1983);* *[4] *Lupton et al. (1980);* *[5] *H. Craig quoted in Des Marais and Moore (1984);* *[6] *Craig et al. (1980).*

mid-ocean ridge basalts. O'Nions and Oxburgh (1983) further suggest that about 90% of the heat loss through the ocean basin (mainly at mid-ocean ridges) is from the lower enriched mantle, while the helium removal from the lower mantle is impeded at the boundary of the lower and higher mantles. Their model predicts a much higher ^{3}He/heat ratio at hotspots than at mid-ocean ridges as the former taps the lower mantle helium more efficiently. The results of this study are compatible with the above models. The rate of magma eruption at hotspots is smaller by an order of magnitude than that at mid-ocean ridges (Ito *et al.*, 1983). Therefore, the present results also imply that the mantle flux of helium and carbon dioxide at both sites could be of equal magnitude.

In the Galapagos Rift hotspring fields, the depletion of sulfide-forming metals such as nickel and cobalt in the fluids is suggested to be the result of sulfide precipitation in subsurface reducing zones (Edmond *et al.*, 1979). The existence of sulfide-forming zones beneath the Loihi summit has been anticipated from the trace element distribution in the nontronite-geothite deposits (De Carlo *et al.*, 1983). In light of these studies, the large concentrations of nickel and cobalt at station 29 may be interpreted as the result of the circulation of oxygenated seawater into the reducing zones, dissolving sulphides or simply incorporating sulphide particles. Recent talus deposits cover a wide area of the summit, including the eastern slope of the large pit crater below station 29; fractures and fissures are actively forming on the Loihi summit through which seawater may reach the sulphide-bearing zones. Alternatively, the incorporation of sulphide particles in the plume at this site may be an indication of high-temperature "smoker" chimneys missed by the CTD surveys

Conclusions

This study demonstrates that the Loihi summit is actively emitting hydrothermal plumes rich in helium, methane, iron and manganese. The depth profiles of these hydrothermal tracers in the water column above the summit and the temperature anomalies in the bottom water suggest that at least two different vent fields exist on the southern part of the summit caldera and one on the northern part. The warm sites are covered with yellowish- to reddish-brown sediments or sediment-coated broken pillows, through which warm water may be emerging out forming chimneys and veins. In addition, subsurface sulphide precipitates are also suggested by a large nickel and cobalt anomaly found at one of the hydrocast stations.

The ^{3}He/heat and CO_2/heat ratios at Loihi and probably at other hotspot volcanoes are one to two orders of magnitude greater than those at mid-ocean ridge spreading centers, in harmony with the current idea that the hotspot volcanism taps more primitive mantle. The large excess of carbon dioxide in the plume produces a pH anomaly which could be utilized as a sensitive tracer for at least hotspot hydrothermal plumes. These results warrant more detailed studies of the Loihi hydrothermal fields, including studies with manned submersibles.

Acknowledgments—We thank the members of "Delphinus Expedition" for their participation in sampling and routine shipboard analyses, the officers and crew of the R/V Hakuho Maru for their help in shipboard operations, T. Doughetry of the Hawaii Undersea Research Laboratory for maintenance of the land stations of the Mini-Ranger navigation system, W. Giggenbach of the Department of Scientific and Industrial Research, New Zealand for his help in the improvement of the gas chromatographic analysis of methane, and K. Hasegawa for manuscript preparation. This research was partially supported by the Grant in Aid for the Scientific Research, Nos. 60221006 and 60430010, from the Ministry of Education, Science and Culture of Japan to the University of Tokyo, and the NOAA National Undersea Research Program at the University of Hawaii, Hawaii Undersea Research Laboratory. Hawaii Institute of Geophysics contribution No. 1841.

References

Akagi, T. and Haraguchi, H. (1984) Distributions and behaviors of trace heavy metals in the Tama river estuary and Tokyo Bay. *Chikyu Kagaku* (Geoche-

mistry) **18**, 81–88 (Japanese).

Akagi, T., Fuwa, K. and Haraguchi, H. (1985) Simultaneous multi-element determination of trace metals in seawater by inductively-coupled plasma atomic emission spectrometry after coprecipitation with gallium. *Anal. Chim. Acta* **177**, 139–151.

Craig, H. and Lupton, J. E. (1976) Primordial neon, helium and hydrogen in oceanic basalts. *Earth Planet. Sci. Lett.* **31**, 369–400.

Craig, H., Lupton, J. E., Welhan, J. A. and Poreda, R. (1978) Helium isotope ratios in Yellowstone and Lassen Park volcanic gases. *Geophys. Res. Lett.* **5**, 897–900.

Craig, H., Welhan, J. A., Kim, K. -R., Poreda, R. and Lupton, J. E. (1980) Geochemical studies of the 21°N EPR hydrothermal fluids. *EOS* **61**, 992.

Craig H., Kim, K. -R. and Rison, W. (1984) Easter Island hotspot: I. Bathymetry, helium isotopes, and hydrothermal methane and helium. *EOS* **65**, 1140.

De Carlo, E. H., McMurtry, G. M. and Yeh, H. -W. (1983) Geochemistry of hydrothermal deposits from Loihi submarine volcano, Hawaii. *Earth Planet. Sci. Lett.* **66**, 438–449.

Des Marais, D. J. and Moore, J. G. (1984) Carbon and its isotopes in mid-oceanic basaltic glasses. *Earth Planet. Sci. Lett.* **69**, 43–57.

Edmond, J. M., Measures, C., Mangum, B., Grant, B, Sclater, R. R., Collier, R., Hudson, A., Gordon, L. I., and Corliss, J. B. (1979) On the formation of metal-rich deposits at ridge crests. *Earth Planet. Sci. Lett.* **46**, 19–30.

Gamo, T. and Horibe, Y. (1980) Precise determination of dissolved gases in sea water by shipboard gas chromatography. *Bull. Chem. Soc. Jpn.* **53**, 2839–2842.

Horibe, Y., Kim, K. -R. and Craig, H. (1983) Off-ridge submarine hydrothermal vents: Back-arc spreading centers and hotspot seamounts. *EOS* **64**, 724.

Ito, E., Harris, D. M. and Anderson, Jr., A. T. (1983) Alteration of oceanic crust and geologic cycling of chlorine and water. *Geochim. Cosmochim. Acta* **47**, 1613–1624.

Jenkins, W. J., Edmond, J. M. and Corliss, J. B. (1978) Excess ^{3}He and ^{4}He in Galapagos submarine hydrothermal waters. *Nature* **272**, 156–158.

Kaneoka, I. and Takaoka, N. (1980) Rare gas isotopes in Hawaiian ultramafic nodules and volcanic rocks: constraint on genetic relationships. *Science* **208**, 1366–1368.

Kim, K. -R. (1983) Methane and radioactive isotopes in submarine hydrothermal systems. PhD Thesis, University of California at San Diego.

Kurz, M. D., Jenkins, W. J., Hart, S. R. and Claque, D. (1983) Helium isotopic variations in volcanic rocks from Loihi Seamount and the Islands of Hawaii. *Earth Planet. Sci. Lett.* **66**, 388–406.

Lilley, M. D., Baross, J. A. and Gordon, L. I. (1983) CH_4, H_2, CO and N_2O in submarine hydrothermal vent waters. *Nature* **300**, 48–50.

Lilley, M. D., Baross, J. A. and Gordon, L. I. (1983) Reduced gases and bacteria in hydrothermal fluids: The Galapagos spreading center and 21°N East Pacific Rise. *Hydrothermal Processes at Seafloor Spreading Centers* 411–449. Edited by P.A.Rona, K. Boström, L. Laubier and K. L. Smith, Jr. Plenum Press, New York.

Lupton, J. E., Weiss, R. F. and Craig, H. (1977) Mantle helium in hydrothermal plumes in the Galapagos Rift. *Nature* **267**, 603–604.

Lupton, J. E., Klinkhammer, G. P., Normark, W. R., Hayman, R., Macdonald, K. C., Weiss, R. F. and Craig, H. (1980) Helium-3 and manganese at the 21°N East Pacific Rise hydrothermal site. *Earth Planet Sci. Lett.* **50**, 115–127.

Malahoff, A., McMurtry, G. M., Wiltshire, J. C. and Yeh, H. -W. (1982) Geology and chemistry of hydrothermal deposits from active submarine volcano Loihi, Hawaii. *Nature* **298**, 234–239.

Malahoff, A. (1986) The geology of the summit of Loihi submarine volcano, Hawaii. *U.S. Geol. Surv. Prof. Pap.* **1350**, Chapt 6.

Michard, G., Albareide, F., Michard, A., Minster, J. -F., Charlou, J. -L and Tan, N. (1984) Chemistry of solutions from the 13°N East Pacific Rise hydrothermal site. *Earth Planet. Sci. Lett.* **67**, 297–307.

Moore, J. G., Claque, D. A. and Normark, W. R. (1982) Diverse basalt types from Loihi Seamount, Hawaii. *Geology* **10**, 88–92.

O'Nions, R. K. and Oxburgh, E. R. (1983) Heat and helium in the Earth. *Nature* **306**, 429–431.

Rison, W. and Craig, H. (1983) Helium isotopes and mantle volatiles in Loihi Seamount and Hawaiian Island basalts and xenoliths. *Earth Planet. Sci. Lett.* **66**, 407–426.

Sano, Y., Urabe, A., Wakita, H., Chiba, H. and Sakai, H. (1985) Chemical and isotopic compositions of gases in geothermal fluids in Iceland. *Geochem. J.* **19**, 135–148.

Schaule, B. K. and Patterson, C. C. (1981) Lead concentrations in the northeast Pacific: evidence for global anthropogenic perturbations. *Earth Planet. Sci. Lett.* **54**, 97–116.

Skirrow, G. (1974) The dissolved gases - carbon dioxide. *Chemical Oceanography* **2**, 1–192. Edited by J. P. Riley and G. Skirrow, Academic Press: London.

Weiss, R. F., Lonsdale, P., Lupton, J. E., Bainbridge, A. E. and Craig, H. (1977) Hydrothermal plumes in the Galapagos Rift. *Nature* **267**, 600–603.

Welhan, J. A. and Craig, H. (1979) Methane and hydrogen in East Pacific Rise hydrothermal fluids. *Geophys. Res. Lett.* **6**, 829–831.

Welhan, J. A. and Craig, H. (1983) Methane, hydrogen and helium in hydrothermal fluids at 21°N on the East Pacific Rise. *Hydrothermal Processes at Seafloor Spreading Centers* 391–409. Edited by P. A. Rona, K. Boström, L. Laubier and K. L. Smith, Jr. Plenum Press, New York.